

Coupling effects of stress and ion irradiation on the mechanical behaviors of copper nanowires

YANG ZhenYu^{1*}, JIAO FeiFei¹, LU ZiXing¹ & WANG ZhiQiao²

¹ School of Aeronautic Science and Engineering, BeiHang University, Beijing 100191, China;

² School of Engineering and Technology, China University of Geosciences, Beijing 100083, China

Received November 7, 2012; accepted January 8, 2013

By using molecular dynamics simulations, we studied the ion irradiation induced damage in mechanically strained Cu nanowires and evaluated the effects of damage on the mechanical properties of nanowires. The stresses in the pre-strained nanowires can be released significantly by the dislocation emission from the cascade core when the strain is greater than 1%. In addition, comparison of the stress-strain relationships between the defect-free nanowire and the irradiated ones indicates that ion irradiation reduces the yield strength of the Cu nanowires, and both the yield stress and strain decrease with the increase of irradiation energy. The results are consistent with the microscopic mechanism of damage production by ion irradiation and provide quantitative information required for accessing the stability of nanomaterials subjected to mechanical loading and irradiation coupling effects.

ion irradiation, nanowires, molecular dynamics, vacancy, dislocation

PACS number(s): 31.15.xv, 61.72.J-, 61.82.-d, 62.23.Hj, 62.25.-g

Citation: Yang Z Y, Jiao F F, Lu Z X, et al. Coupling effects of stress and ion irradiation on the mechanical behaviors of copper nanowires. *Sci China-Phys Mech Astron*, 2013, 56: 498–505, doi: 10.1007/s11433-013-5008-6

1 Introduction

Nanowires have been known for their unique physical properties as compared to bulk materials [1,2], becoming critical building blocks of nanoelectromechanical systems (NEMS) [3]. The behaviors of nanomaterials under irradiation have attracted increasing research focus [4–7], for the nanostructured materials in general might have exceptional irradiation resistance for their large free surface to volume ratio [8,9]. In addition, Nanowires are recently reported to be developed for radiation detection applications [10]. The effects of particle irradiation on the properties of materials can be detrimental or beneficial [11].

To design robust materials, it is critical to understand the way that radiation-induced defects alter the mechanical

properties on a fundamental level. Kiener et al. [12] recently performed *in situ* strength measurements of nanoscale irradiated copper in a transmission electron microscope (TEM) and showed that the strength of samples with dimension above ~400 nm is controlled by dislocation-irradiation defect interactions, while size-dependent strength results from dislocation source limitation for the samples below ~400 nm. By using molecular dynamics and density-functional theory simulations, Holmstrom et al. [13] studied the radiation hardness of mechanically strained carbon nanotubes and silicon nanowires and found the radiation hardness of all these structures decreases with strain. The threshold displacement energy in hexagonal Si nanowires with a <111>-oriented axis and with all side facets being <112> was also recently studied [14]. In addition, defect formation energies in Cu nanowires have been studied with the classical MD simulations [15]. It was predicted that the formation

*Corresponding author (email: zzyang@buaa.edu.cn)

energy of vacancies is the lowest in the middle of the nanowires and the formation energy of adatoms decrease with decreasing nanowires diameter. Zou et al. [16] have studied the damage caused by low-energy ion irradiation on copper nanowires and observed the surface vacancies prefer to remain on (100) plane and adatoms on (110) plane. Although a great deal of research has been focused on the mechanical behaviors of defect-free nanowires [17–19] and nanowires with pre-existing defects [20,21], there is very little fundamental knowledge of how metal nanowires respond to ion bombardment with mechanical load coupling effects.

Radiation damage in metals has been extensively studied by experiments and simulations. However, the microscopic processes that underline those effects are not entirely understood, limiting the ability to predict the consequences of irradiation. The response of nanowires to irradiation is not well understood, because of relatively little experimental and little theoretical work on these systems [6]. MD simulations are well suited to study the irradiation processes, as the time scales of the collisions and energy dissipation are on the order of a few picoseconds. Energetic particle irradiation removes atoms from their lattice sites during a collision cascade in a few picoseconds. In order to shed light on the intrinsic mechanisms of pre-strained metal nanowires under irradiation, we simulated <111>-oriented Cu nanowires with a specific strain and an energetic ion irradiation. The defects produced by irradiation in the nanowires are analyzed according to the evolution of inside nanostructures. In addition, the effects of pre-existing strain on the ion irradiation induced damage are simulated and discussed. Consequently, we demonstrate that the ion irradiation can release the pre-existed stress in nanowires dramatically at certain conditions. At last, comparison between the behaviors of defect-free and irradiated nanowires are made to understand how ion irradiation induced defects influence the mechanical properties of Cu nanowires

2 Molecular dynamics simulation methods

The circular nanowires with diameters of 12 nm and axial length of 38.8 nm were cut from perfect bulk crystal. All nanowires used in the following simulations were <111> oriented and are periodic in axial direction with total 269224 atoms. The embedded atom method (EAM) potential developed by Mishin et al. [22] was used to describe the interatomic interaction between Cu atoms, which has been recently used in the MD simulation of radiation damage near grain boundaries in Cu nanomaterials [23]. In the embedded-atom method, the total energy of an atomistic system is represented as [22]:

$$E = \frac{1}{2} \sum_{ij} V(r_{ij}) + \sum_i F(\bar{\rho}_i), \quad (1)$$

where $V(r_{ij})$ is a pair potential as function of distance r_{ij}

between atoms i and j , and F is the embedding energy as a function of the host electron density $\bar{\rho}_i$ induced at site i by all other atoms in the model.

In addition, Ziegler, Biersack and Littmark (ZBL) potential [24] is adopted to describe the repulsion behavior at short distance. For the ZBL potential, the potential can be written as:

$$V_{ij}^{ZBL} = \frac{1}{4\pi\epsilon_0} \frac{Z_1 Z_2 e^2}{r_{ij}} \phi(r_{ij}/a), \quad (2)$$

with Z_1, Z_2 as the number of protons in each nucleus, e as the electron charge and ϵ_0 as the permittivity of vacuum. The second part $\phi(x)$ is the ZBL universal screening function, which is represented as:

$$\phi(x) = 0.1818e^{-3.2x} + 0.5099e^{-0.9423x} + 0.2802e^{-0.4029x} + 0.02817e^{-0.2016x}, \quad (3)$$

in which

$$a = \frac{0.8854a_0}{Z_1^{0.23} + Z_2^{0.23}}, \quad (4)$$

with a_0 being the Bohr radius, and the coefficients provided elsewhere [24].

The pairwise portion of EAM interatomic potential was smoothly splined to the ZBL potential for interatomic distances less than 0.75 Å, with a Fermi-like function:

$$V_{ij} = (1 - f_F(r_{ij}))V_{ij}^{ZBL} + f_F(r_{ij})V_{ij}^{EAM}, \quad (5)$$

where

$$f_F(r_{ij}) = \frac{1}{1 + e^{-A_F(r_{ij}-r_c)}}, \quad (6)$$

in which, A_F controls how sharp the transition is between the two potentials, and r_c is essentially the cut off for the ZBL potentials. Implementation of the ZBL potential for short-range interatomic interactions enables simulations of response to ion bombardment and provides a realistic description of defect properties, melting temperature and displacement characteristics [8,13–15].

After cutting out, the nanowires were first relaxed using the conjugate gradient method and then equilibrated at 300 K using the Nose-Hoover thermostat for 50 ps to approach zero stress in axial direction. Then the nanowires were loaded to the prescribed strain ranging from –4% to 4%, in which the Cu nanowires are elastically deformed. After the mechanical deformation, the nanowires were equilibrated with an additional 50-ps-run with the length fixed. The cascade was initiated by assigning corresponding kinetic energy to a selected surface atom, as shown in Figure 1. The

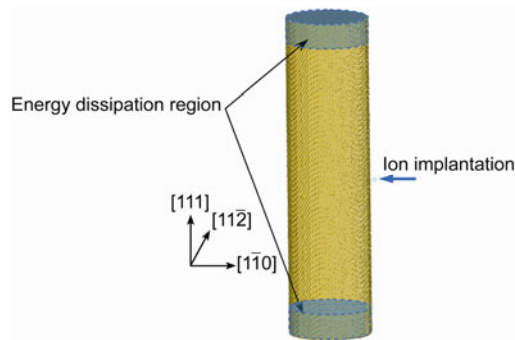


Figure 1 Atomistic model for ion irradiation on $\langle 111 \rangle$ Cu nanowires. The velocities of atoms in the shadow region are scaled for energy dissipation in the cascade simulation.

incident directions of ions are normal to the free surface of nanowire in $[1\bar{1}0]$ direction. After ion irradiation was introduced, the systems were relaxed using microcanonical ensemble (NVE), with ten layers of atoms of the nanowires ends set as the energy dissipation region, where the temperature is fixed at 300 K. Dynamics time step control was applied to ensure that the displacement during each time does not exceed 0.05 \AA . Any atom at a distance of 5 \AA from the surface was considered sputtered and was excluded in the ongoing simulation. The structures of the nanowires were monitored in the real time, and the simulations were stopped until no more structural changes occurred in the nanowires and energy convergence approached. Primary knock-on atom (PKA) energies of 1–10 keV were used for simulations.

Electronic energy loss processes during the collision cascade lead to dilution of displacement production and local heat generation that may enhance in-cascade relaxation. These effects are beyond the scope of this work. However, binary collision approximation calculations indicate that at energies below 10 keV, electronic energy loss is typically an order of magnitude less than nuclear energy loss [25].

All the MD simulations presented in this paper were performed using the large-scale atomic molecular massively parallel simulator (LAMMPS) [26]. The average stresses in the atomistic systems were calculated using the virial theorem [27]. The snapshots of the deformation were recorded and then processed by Atomeye [28].

3 Results and discussion

3.1 Ion irradiation induced damage in nanowires

In presenting the results, we first look at the damage evolution in the pre-strained Cu nanowires by ion irradiation then examine the atomic mechanism in details. Initially, the PKA is not triggered, and the structure of the Cu nanowire is a perfect crystal without any atoms displaced from the lattice

sites. Starting from perfect FCC structure, lattice sites near the surface are molten because of the high energy deposited into the nanowire, as shown in Figure 2, which shows the dynamic process of the nanostructures evolution in nanowires under a 5-keV radiation. At 0.015 ps, the PKA has penetrated about 1 nm distance from the surface into the nanowire, but the small collision cascades are mainly focused near the surface with several atoms sputtered to the surface. There is no obvious difference between the strained nanowires and the free nanowires. At 0.05 ps, according to the velocity of the PKA, the PKA has penetrated almost half of the cross section of the nanowire, inducing many collisions in the nanowires. More atoms sputtering and local melting are observed and the displacements of the strained nanowires are more obvious. At 0.5 ps, the collision cascade has spread through almost the entire cross section, with many atoms driven to free surface from the impact region due to the high temperature and pressure there. The regular lattices at the cascade core have transformed into amorphous region. The discontinuous displacement of the atoms at the nanowires surface can be observed in the mechanically strained nanowires, which indicates the dislocation nucleation and propagation. According to the displacement distribution of the free nanowire surface, no dislocation is nucleated. At 50 ps, some of those disturbed atoms recover to regular lattice sites when the cascade cools down, and others just reside at free surface and become surface adatoms. For the mechanically strained nanowires, the discontinuous distributions of the displacement at the wire surface demonstrate the movement of the dislocations. In addition, many vacancies are created in the nanowire, as shown in Figure 3, because of the sputtered atoms which are emitted from the free surface to the vacuum. Several isolated vacancies and cluster defects are also observed, meaning that the

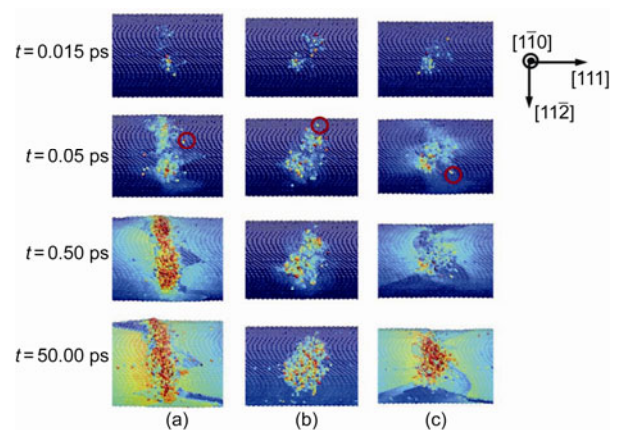


Figure 2 Atomic configuration of Cu nanowires containing a 5 keV cascade coupling with strains of (a) -4% , (b) 0 and (c) 4% . The atoms are colored with the current displacement from its original coordinates, and the figures are projected onto (110) plane. The dark blue indicates the smallest displacement 0 \AA and the red for the largest displacement 10 \AA . The red circles highlight the adatoms on the nanowires surface. The sputtered atoms with displacement over 10 \AA are not shown here.

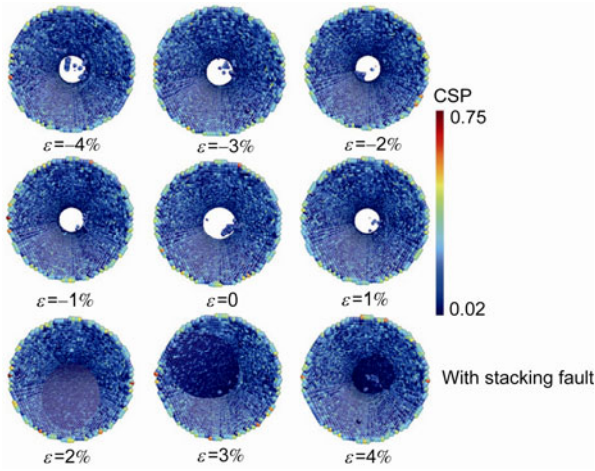


Figure 3 Final equilibrium structures of Cu nanowires after annealing of the ion collision, with atoms colored by central symmetry parameters (CSP).

ballistic collision contributes to the defect production.

Figure 3 shows the final equilibrium structures in the nanowires with pre-strain range from -4% to 4% after a 5-keV ion irradiation. For the nanowires with compressive pre-strain, only point defects and cluster defects left in the nanowires after equilibrium. Similarly, only point defects are observed in nanowire with pre-strain of 1% . But the situation is different for nanowires with pre-strain equal or greater than 2% , where stacking faults in $\{111\}$ planes are formed across the nanowire section. Several vacancies can also be observed at the both sides of the stacking faults. Zhang et al. [29,30] suggested that using energetic beams or the combination of mechanical torsion and local melting of nanowires with subsequent solidification can induce twin boundaries into nanowires. Consequently, it is possible to tune the mechanical behaviors of nanomaterials by changing the nanostructure inside with using ion irradiation.

3.2 Stress release by ion irradiation

To understand the response of mechanically strained nanowires to irradiation, we recorded the change of stress in nanowires along the axial with variation of time. The axial stresses in nanowires were recorded every 100 steps and the stress-time curve was filtered with a 100-points fast Fourier transform (FFT) smoothing to eliminate the thermal noise. Figure 4(a) shows the evolution of ion irradiation induced nanostructures in the Cu nanowire with a tensile strain of 4% . At the beginning of the collision, leading dislocations nucleate at the site where the energetic ion deposited. All of the dislocations slip in $\{111\}$ planes are finally absorbed by the free surface of nanowire. Most of the stacking faults caused by the partial dislocations were finally eliminated by a trailing dislocation, but one of the stacking faults remained in the nanowire. Actually, the movement of the dislocations in the Cu nanowires is driven by both pre-existed stress and bombardment of ion. The evolution of axial stress with time is presented in Figure 4(b). When the Cu nanowire is stretched with a strain of 1% , there is no obvious difference between the stresses before and after ion implantation, because no dislocation is triggered by ion irradiation thus the stress cannot be released by dislocation slip. For the nanowires with pre-existed strain greater than or equal to 2% , the axial stress is obviously released by the ion implantation in the first 5 ps. In addition, it is interesting to note that the stress release is more remarkable in nanowires with higher strain. The damage and axial stress evolution of the compressed nanowire under ion irradiation are presented in Figure 5. The evolution of the inside structures of a compressed nanowire is shown as Figure 5(a), which has a compressive strain of -4% before the ion irradiation. When the compressive strain is not greater than 1% , only point defects diffusion is observed but no dislocation emission from cascade core. Consequently, the axial stresses show no

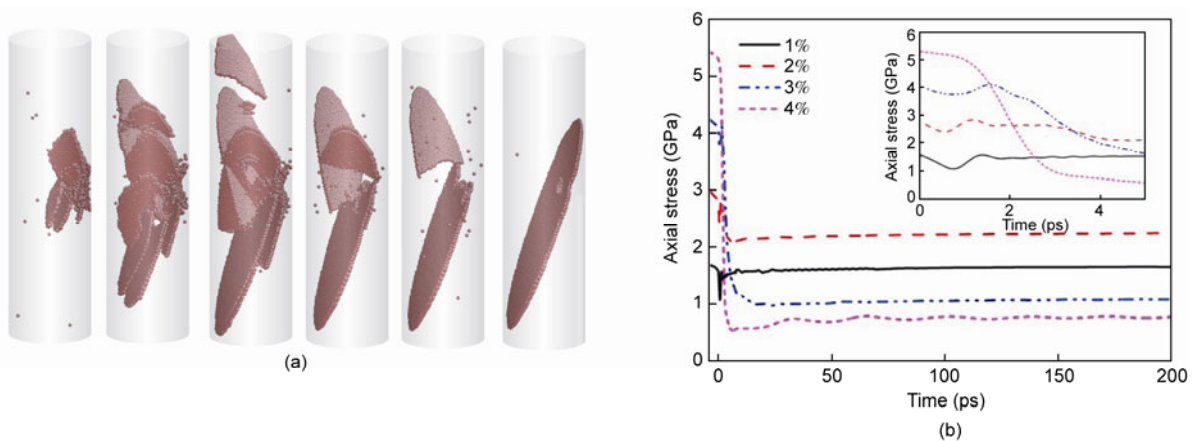


Figure 4 (a) 5 keV PKA induced damage evolution in nanowire with pre-existed strain of 4% . The red balls represent atoms in HCP structure. The cylinder denotes the initial nanowire surface. (b) Stress change with the time, where the ion collision is triggered at 0 ps. The evolution of the stress in the first 5 ps is shown in the upper right corner panel.

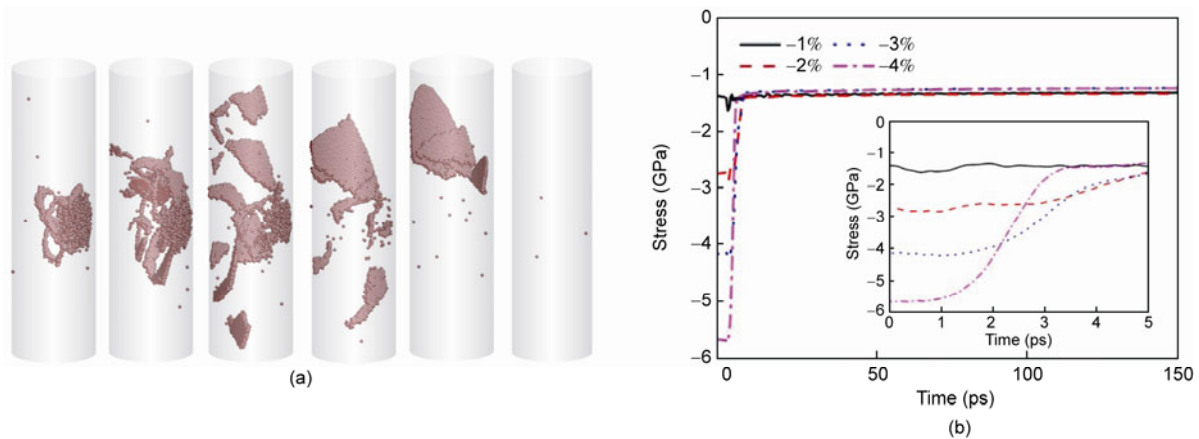


Figure 5 (a) 5 keV PKA induced damage evolution in nanowire with pre-existed strain of -4% . The red balls represent atoms in HCP structure. The cylinder denotes the initial nanowire surface. (b) Stress change with the time, where the ion collision is triggered at 0 ps. The evolution of the stress in the first 5 ps is shown in the lower right corner.

remarkably change after ion irradiation, as shown in Figure 5(b). For the nanowires with compressive pre-strain of -2% to -4% , partial dislocations nucleate at the cascade core and lead stacking faults, followed with trailing dislocations, as shown in Figure 5(a). After all the dislocations are absorbed by the surfaces of nanowires, only point defects and clusters are left in the nanowires. Finally, the axial compressive stresses in nanowires are released to almost the same level (about -1.4 GPa) by Shockley dislocations slip in $\{111\}$ planes.

In addition, the residual stresses in the nanowires with irradiation energy changing from 2 keV to 10 keV are illustrated in Figure 6. The red circular represents the residual stress in nanowire with tensile strain of 4% and the dark square for the nanowire with compressive strain of -4% . The residual stresses in nanowire decrease with increase the PKA energy and approach to 0.5 GPa and -0.4 GPa, respectively.

3.3 The mechanical behaviors of irradiated nanowires

To understand how ion irradiation induced defects influence the mechanical properties of Cu nanowires, the stress-strain responses of the irradiated free nanowires with axial loading were calculated by using the same method as described elsewhere [17,18].

Figure 7 shows the ion irradiation induced damage in the nanowires with different PKA energy. Apparently, 2-keV ion irradiation results in about 4 vacancies and a self-interstitial atom in the nanowire, which are close to the surface. More vacancies are observed when the irradiation energy increase to 5 keV, but no self-interstitial atoms. An ion irradiation with energy high up to 10 keV can lead to dislocation loop and dispersed point defects. The comparison of the tensile behaviors between the free Cu nanowires before and after ion irradiation is illustrated in Figure 8. It appears that

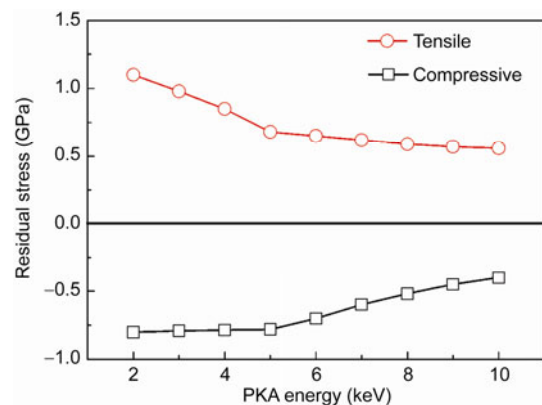


Figure 6 Residual stress in nanowires with pre-existed strain of 4% and -4% changes with the energy of ion irradiation.

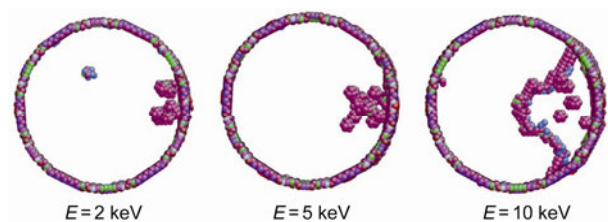


Figure 7 Typical residual defects in free nanowires under ion irradiation with different energies. The atoms are colored according to the coordination number. The perfect FCC atoms are removed for clarity. The red balls represent the atoms with coordination number of 11.

the MD simulation results show that the ion irradiation reduces the yield strength of the Cu nanowire, and both the yield stress and yield strain decrease with the increase of the irradiation energy. Ren et al. [31] have shown that the ion irradiation can lead to the softening of a 3-nm-diameter GaN nanowire, meaning that the defects in nanowire cause a small decrease in the Young's modulus value, which may lead to larger softening by higher fluences ($(1 \text{ ion})/(30 \text{ nm}^2) \approx 3.3 \times 10^{12} \text{ ions/cm}^2$). Simulations on the 12-nm-diameter Cu

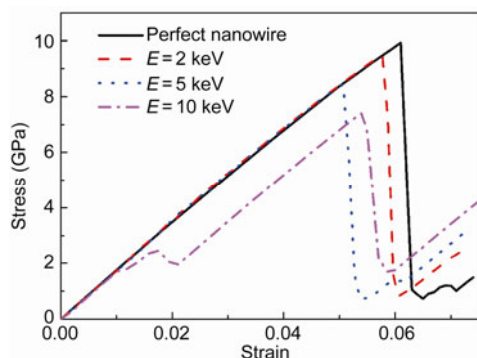


Figure 8 (Color online) Comparison of the tensile behaviors between the Cu nanowires before and after ion irradiation with the different PKA energies.

nanowires show that the effects of defects on Young's modulus are not apparent, but the yield stress is lowered by the ion irradiation. The Cu nanowires in this paper has 16 times cross-sectional area of the 3-nm-diameter GaN nanowire, so the influence of the defects on the Young's modulus of Cu nanowire is not as apparent as that on GaN nanowire [31], which indicates the size effects of the ion irradiation on nanowires. In addition, the results show that the presence of vacancies lowers the yield stress, and a higher concentration may cause a higher deviation from the yield point with no vacancies, which was predicted to be a weak power law relationship [32]. Comparing with the other cases, the nanowire irradiated by a 10-keV ion shows the lowest initial yield stress and strain hardening can be observed from the tensile stress-strain curve, which indicates the plastic deformation mechanism of this nanowire differs from others.

A dynamic observation of the typical dislocation activities during the initial yielding deformation of the defect-free nanowire is shown in Figure 9. The deformation begins with a dislocation emitting from the surface and then is captured



Figure 9 (Color online) Initial yielding deformation of the defect-free Cu nanowires. At the elastic limit (a), a dislocation nucleates at the surface and emits across the nanowire section (b), and finally absorbed by the surface (c). HCP atoms are shown in red in this figure and following figures.

by surface. The dislocation gliding on the $\{111\}$ plane leads to the sharp decline of the tensile stress. While, the ion irradiation changes the regular lattices structure of the wire and results in vacancies and defect clusters. Figure 10 shows the incipient plastic deformation of the nanowire subjected to a 5-keV irradiation then a tensile loading. Two leading partial dislocations nucleate simultaneously at the cascade core and propagate across the nanowire section, indicating the lower resistance of the nanowire to tensile loading. The irradiation energy increasing to 10 keV, the defective structure in the nanowire is different, as shown in Figure 7. The continuous snapshots of initial yielding deformation of the nanowire are illustrated in Figure 11. Upon tensile loading of the Cu nanowire with a 10-keV irradiation, the first leading partial dislocation is nucleated from the dislocation loop induced by the irradiation and moves around the nucleation site anticlockwise and forms a stacking fault across the nanowire section. After, a trailing partial dislocation is emitted from the same site and moves around the "pin" in counter-clockwise direction and finally moves out of the nanowire. The "pin" effects of the defect cluster on the dislocation may attribute to the strain hardening behavior. The mechanical response of a nanomaterial because of irradiation is predominantly controlled by the evolution of the irradiation-induced nanostructure. This in turn is driven not by the total number of displaced atoms but the small fraction of point defects that avoid annihilation by mutual recombination.

To explore the structural changes in nanowires, which induced by ion irradiation and stress coupling effects, the displacement coloring method is employed to observe the movement of the surface atoms, such as atoms sputtering and local melting. In addition, the CSP coloring method is adopted for measure of local lattice disorder. In contrast to

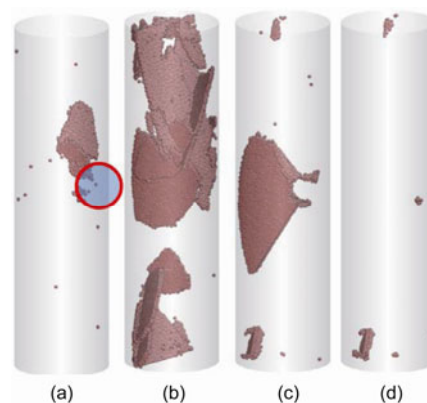


Figure 10 (Color online) Incipient tensile plastic deformation of the nanowire after a 5-keV ion irradiation. The circle indicates the cascade core. (a) Two leading partial dislocations nucleate at the cascade core at the elastic limit with stacking faults left behind. (b) Initial leading dislocations propagate across the nanowire section and more partial dislocations emit from the surface and glide on the $\{111\}$ slip planes. (c) Most of the dislocations are absorbed by the surface. (d) Only cluster defects left in the nanowire after all the dislocation moving out of the nanowire.

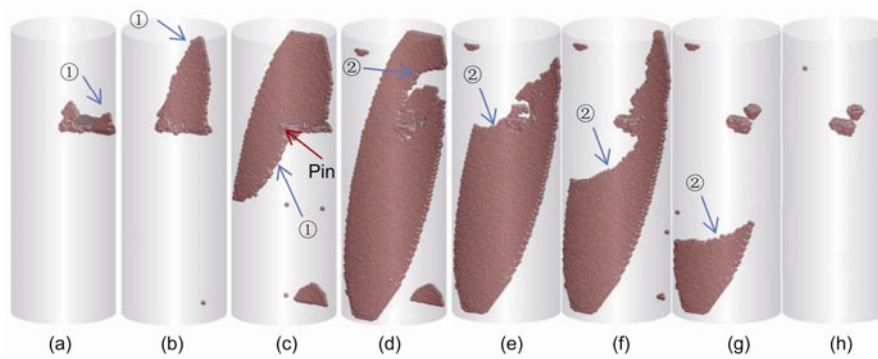


Figure 11 (Color online) Incipient plastic deformation of the nanowire after a 10-keV ion irradiation then subjected to tensile loading. Leading partial ① nucleates at the elastic limit (a), then propagates from (b) to (c), where leading partial moves around the “pin”. The dislocation is absorbed by surface at (d) and trailing partial ② nucleates at the cascade core. Approximate circular motion of trailing partial ② can be observed from (e) to (g), and finally moving out of the nanowire (h), leaving only defect clusters in the nanowire.

the CSP method, the HCP coloring is based not on the distance between particles but the angles and is stable against temperature boost, so it is helpful to display the formation of stacking faults in irradiated nanowires. The coordination number coloring is another method to show the defect atoms in crystals. With this method, the point defects and dislocation line can be clearly observed. Combing the HCP coloring and coordination number coloring, it is possible to characterize the orientation of the dislocation movement. These types of coloring method are combined together are useful to collect the detail information of the nanostructures evolution inside nanowires.

4 Conclusions

The effects of stress and irradiation coupling on the mechanical behaviors of pre-strained nanowires were studied with using MD simulations. The results show that the stress in stretched or compressed nanowires can be released by ion irradiation. How much the stress can be released is determined by both the stress level and the KPA energy. For the pre-strained nanowire with the absolute strain above 1%, a 5-keV ion irradiation can lead to many dislocations nucleate at the cascade core, thus the stress is released by the dislocations slip. The compressed nanowires are preferred to keep vacancies or cluster defects after ion irradiation, while the stretched nanowires are found to have a stacking fault left after the ion irradiation. Finally, the defects induced by ion irradiation in the Cu nanowire cause an apparent decrease of the yield stress of the nanowires. The simulation results suggest a possible way to change the intrinsic structures of nanowires by using energetic beams to tune the mechanical properties of nanomaterials, such as to eliminate the residual stress in the metallic nanosystems. In addition, nanowires can be developed for radiation detection applications [10] for their physical properties changed during the ion irradiation. Properties such as widely tunable mechani-

cal properties and electronic bandgaps [4] of nanowires promise to provide new approaches for radiation detection.

This work was supported by the National Natural Sciences Foundation of China (Grant Nos. 11002011, 10902111 and 10932001) and Fundamental Research Funds for the Central Universities. In addition, we thank the support from the High Performance Computing Center of BUAA.

- 1 Tosatti E, Prestipino S, Kostlmeier S, et al. String tension and stability of magic tip-suspended nanowires. *Science*, 2001, 291: 288–290
- 2 Wu B, Heidelberg A, Boland J J. Mechanical properties of ultrahigh-strength gold nanowires. *Nat Mater*, 2005, 4: 525–529
- 3 Postma H W C, Kozinsky I, Husain A, et al. Dynamic range of nanotube- and nanowire-based electromechanical systems. *Appl Phys Lett*, 2005, 86: 223105
- 4 Talapatra S, Ganesan P G, Kim T, et al. Irradiation-induced magnetism in carbon nanostructures. *Phys Rev Lett*, 2005, 95: 097201
- 5 Zhang Q, Qi J J, Li X, et al. Diameter-dependent internal gain in ZnO micro/nanowires under electron beam irradiation. *Nanoscale*, 2011, 3: 3060–3063
- 6 Krasheninnikov A V, Nordlund K. Ion and electron irradiation-induced effects in nanostructured materials. *J Appl Phys*, 2010, 107: 071301
- 7 Kim Y J, Song J H. Dose rate and irradiation time effects on the shape of Au nanomaterials under proton beam irradiation. *Nanotechnology*, 2007, 18: 445603
- 8 Bai X M, Voter A F, Hoagland R G, et al. Efficient annealing of radiation damage near grain boundaries via interstitial emission. *Science*, 2010, 327: 1631–1634
- 9 Wurster S, Phipps R. Nanostructured metals under irradiation. *Scripta Mater*, 2009, 60: 083–1087
- 10 Chai G, Lupan O, Chow L, et al. Crossed zinc oxide nanorods for ultraviolet radiation detection. *Sensor Actuat A-Phys*, 2009, 150: 184–187
- 11 Wirth B D. How does radiation damage materials. *Science*, 2007, 318: 923–924
- 12 Kiener D, Hosemann P, Maloy S A, et al. *In situ* nanocompression testing of irradiated copper. *Nat Mater*, 2011, 10: 608–613
- 13 Holmstrom E, Toikka L, Krasheninnikov A V, et al. Response of mechanically strained nanomaterials to irradiation: Insight from atomistic simulations. *Phys Rev B*, 2010, 82: 045420

- 14 Hoilijoki S, Holmstrom E, Nordlund K. Enhancement of irradiation-induced defect production in Si nanowires. *J Appl Phys*, 2011, 110: 043540
- 15 Kang J W, Seo J J, Byun K R, et al. Defects in ultrathin copper nanowires: Atomistic simulations. *Phys Rev B*, 2002, 66: 125405
- 16 Zou X Q, Xue J M, Wang Y G. Damage of low-energy ion irradiation on copper nanowire: molecular dynamics simulation. *Chin Phys B*, 2010, 19: 036102
- 17 Yang Z Y, Lu Z X, Zhao Y P. Atomistic simulation on size-dependent yield strength and defects evolution of metal nanowires. *Comput Mater Sci*, 2009, 46: 142–150
- 18 Yang Z Y, Lu Z X, Zhao Y P. Shape effects on the yield stress and deformation of silicon nanowires: A molecular dynamics simulation. *J Appl Phys*, 2009, 106: 023537
- 19 Wu B, Heidelberg A, Boland J J. Mechanical properties of ultrahigh-strength gold nanowires. *Nat Mater*, 2005, 4: 525–529
- 20 Weinberger C R, Cai W. Surface-controlled dislocation multiplication in metal micropillars. *P Natl Acad Sci Usa*, 2008, 105: 14304–14307
- 21 Huang P H, Fang T H, Chou C S. The coupled effects of size, shape, and location of vacancy clusters on the structural deformation and mechanical strength of defective nanowires. *Curr Appl Phys*, 2011, 11: 878–887
- 22 Mishin Y, Mehl M J, Papaconstantopoulos D A, et al. Structural stability and lattice defects in copper: Ab initio, tight-binding, and embedded-atom calculations. *Phys Rev B*, 2001, 63: 224106
- 23 Bai X M, Voter A F, Hoagland R G, et al. Efficient annealing of radiation damage near grain boundaries via interstitial emission. *Science*, 2010, 327: 1631–1634
- 24 Ziegler J F, Biersack J P, Littmark U. *The stopping and range of ions in solids*. New York: Pergomon, 1985. 34–36
- 25 Devanathan R, Corrales L R, Weber W J, et al. Molecular dynamics simulation of defect production in collision cascades in zircon. *Nucl Instrum Meth B*, 2005, 228: 299–303
- 26 Plimpton S. Fast parallel algorithms for short-range molecular dynamics. *J Comput Phys*, 1995, 117: 1–19
- 27 Zhou M. A new look at the atomic level virial stress: on continuum-molecular system equivalence. *Proc R Soc Lond A Mat*, 2003, 459: 2347–2392
- 28 Li J. AtomEye: an efficient atomistic configuration viewer. *Model Simul Mater Sc*, 2003, 11: 173–177
- 29 Zhang Y, Huang H. Controllable introduction of twin boundaries into nanowires. *J Appl Phys*, 2010, 108: 103507
- 30 Zhang Y, Huang H. Twin Cu nanowires using energetic beams. *Appl Phys Lett*, 2009, 95: 111914
- 31 Ren W, Kuronen A, Nordlund K. Molecular dynamics of irradiation-induced defect production in GaN nanowires. *Phys Rev B*, 2012, 86: 104114
- 32 Njeim E K, Bahr D F. Atomistic simulations of nanoindentation in the presence of vacancies. *Scripta Mater*, 2010, 62: 598–601